AJNR

Experimental Xenon Enhancement with CT Imaging: Cerebral Applications

Burton P. Drayer, David Gur, Sidney K. Wolfson, Jr and Eugene E. Cook

Experimental Xenon Enhancement with CT Imaging: Cerebral Applications

Burton P. Drayer[1]
David Gur[2]
Sidney K. Wolfson, Jr.[3, 4]
Eugene E. Cook[4]

Xenon-enhanced cranial computed tomography (CT) was used to derive the partition coefficient (λ) and flow rate constant (K) and thus provide a functional neuroanatomic map of local cerebral blood flow in eight nonhuman primates. Sequential CT imaging defined the temporal changes of xenon concentration in arterial blood and brain tissue both during and after xenon inhalation. Several methodologies including clearance, buildup, and in vivo "autoradiography" were used to estimate flow in various brain locales. A typical derived fast flow rate using xenon CT methodology was 85 ml/100 g/min, with a range of 58–108. The in vivo autoradiographic method of defining flow seems more clinically applicable in man. The limitations and potential solutions using CT blood flow techniques are discussed.

[1] Departments of Radiology and Neurology, University of Pittsburgh Health Center, Pittsburgh, PA 15213. Present address: Department of Radiology, Duke University Medical Center, P.O. Box 3808, Durham, NC 27710. Address reprint requests to B. P. Drayer.

[2] Department of Radiology, University of Pittsburgh Health Center, Pittsburgh, PA 15213.

[3] Department of Neurosurgery, University of Pittsburgh Health Center, Pittsburgh, PA 15213.

[4] Division of Surgical Research, Montefiore Hospital of Pittsburgh, Pittsburgh, PA 15213.

The evaluation of regional cerebral blood flow has primarily involved the external monitoring of injected or inhaled radionuclides. Although these radionuclide techniques have proven useful, certain limitations exist, such as limited spatial resolution, extracerebral and recirculation contamination, and fixed partition coefficients.

In order to overcome some of these limitations and advance inhalation applications, cranial computed tomography (CT) has been used to image inhaled nonradioactive xenon gas (atomic number, 54; k-edge, 34.6 keV) [1–6]. The improved spatial resolution provided by advanced CT permits better anatomic specificity, and fast (under 10 sec) scanners enable the rapid serial imaging necessary to monitor the changes in xenon concentration over time. This should allow a quantitative, in vivo determination of blood flow rates in discrete anatomic locations (functional neuroanatomic map) based on the principles of inert gas exchange between blood and tissues set forth by Kety [7, 8]. This study examines the strategies, limitations, and potential solutions involved in the evaluation of regional cerebral blood flow using xenon-enhanced CT scanning.

Technique

Blood flow measurements were made on seven healthy adolescent baboons (*Papio cynocephalus [anubis]*) weighing 7.9–10.3 kg. An eighth animal with moderate restrictive lung disease, but no evidence of neurologic deficit, was also studied.

After sedation with phencyclidine hydrochloride (Sernalyn, Bio-Ceutic Labs., St. Joseph, Mo.), a cuffed endotracheal tube was inserted. Sodium pentothal was administered intravenously as needed throughout the experiments to keep the baboon immobile. Continuous cardiac and respiratory monitoring were routine. An arterial catheter was placed in the femoral artery to permit rapid arterial blood sampling. The cuffed endotracheal tube was connected to a closed ventilation apparatus controlling the inhalation of oxygen and xenon.

A multichannel Corning Analyzer was used to measure PaO_2, $PaCO_2$, and pH of samples drawn from the arterial line and the PO_2 and PCO_2 of the expired air. To enable direct measurements of xenon concentration in arterial blood, a plastic water bath surrounding a fitted, 5 ml syringe holder was fastened to the forehead of the supine animal so that the scanning field contained the central part of the syringe. The syringe contained 2.5 ml of arterial blood drawn about 12 sec prior to each sequential scan.

CT scans were performed using a multipurpose American Science and Engineering (AS&E) scanner with a 512 × 512 matrix and 5 mm collimation. A scan angle of 5° above the orbitomeatal baseline was used in all studies. Exposure factors included a 5 sec scan time, 125 kVp, and 20 mA. Subject motion was not a problem, as a surgical plane of anesthetia was maintained. A nonenhanced CT scan was done before each study to affirm the absence of a neuropathologic process and choose an optimal level for the xenon flow measurements. Pure oxygen was inhaled by the animal until nitrogen was essentially washed out of the respiratory system and tissues as indicated by stable arterial and expired oxygen concentrations.

After the baseline scan, a mixture of 80% xenon/20% oxygen was inhaled for a variable time interval (2–16 min). Serial CT scans were performed at 30–60 sec intervals during xenon buildup and clearance. Fresh arterial blood drawn immediately before scanning was placed in the scanning field. The clearance phase was begun by abruptly discontinuing xenon inhalation and replacing it with oxygen inhalation.

A visual evaluation was based on the CT appearance at routine windows as well as on measure mode (direct and reversal) photographs. A gross analysis of temporal changes in brain and blood attenuation coefficient with xenon enhancement was made. The visual review was also important in choosing specific anatomic locations used for the derivation of numeric information concerning the buildup and clearance of xenon.

The average CT number and the calculated standard deviation in a given volume is an indicator of the type of tissue being investigated and its homogeneity, respectively. When flow studies are carried out, it is important to verify that scanning the "same" slice many times under different anode heat loading and over a relatively long period of time, which may result in slight motion, would yield the same average CT numbers. To verify the stability of the derived CT numbers, the same slice was scanned 10 times over 25 min at various time intervals, and the changes in average CT number for different anatomic areas were compared. In addition, since the arterial blood is drawn about 12 sec before the scan, the leakage or escape of xenon from the syringe was evaluated by sequential scanning of several of the xenon-containing blood syringes over a period of several minutes.

Computation Methods

General Principle

On the basis of the principles of inert gas exchange between blood and tissues set forth by Kety [7, 8], regional cerebral blood flow in the various tissue compartments can be derived from the time-dependent xenon concentration in the arterial blood and in the tissue of interest. For a given compartment i:

$$C_i(t) = f_i \int_0^T C_a(w)e^{-K_i(t-w)}dw, \qquad (1)$$

where C_i and C_a are the tissue and blood xenon concentrations, respectively. K_i is the tissue clearance or buildup rate

constant, and f_i is the flow rate in the compartment;

$$f_i = \lambda_i K_i, \qquad (2)$$

where λ_i is the tissue blood partition coefficient.

The derivation of regional cerebral blood flow from these relationships can be optimized for xenon buildup in the tissue during inhalation, as well as for xenon clearance after termination of xenon inhalation. Methods to optimize statistically the fast and slow blood flow in multicompartmental tissue have been developed for radionuclide studies [9, 10]. Curve-stripping and "autoradiographic" techniques have also been used in an attempt to maximize the information derived from limited numerical data.

Clearance (Washout) Analysis

Four clearance data sets were analyzed using a statistical method similar to that developed for inhalation by Obrist et al. [9]. Because of the limited number of data points, six to nine during a 10 min clearance study, the results were overly sensitive to small variations in CT numbers. Therefore, a simple curve-stripping approach with a first order correction for recirculation was used. After rearrangement, equation (1) can be written as:

$$C_i(t) = [C_i(t_s)e^{-K_i(t-t_s)}] + \left[f_i \int_{t_s}^t C_a(w)e^{-K_i(t-w)}dw \right], \qquad (3)$$

where the first term is a true exponential clearance with no recirculation considerations, and the second term is the contribution from recirculation. The time where analysis is initiated is t_s.

Radionuclide inhalation studies suggest that the major recirculation contribution is in the first minute [9, 11], and that the recommended time to start the analysis is therefore not at termination of inhalation but rather a minute later. All our studies confirm this observation and therefore, t_s was chosen to be 1 min after termination of inhalation.

If one assumes that the xenon concentration in the arterial blood exhibits a mono- or biexponential clearance, $C_a(t)$ can be mathematically expressed using a least square fit of log $C_a(t)$. Once the blood clearance is exponentially characterized, the convolution integral in equation (3) can be solved and the recirculation contribution at any given point in time estimated. For a monoexponential blood clearance:

$$RC_i(t) = \lambda_i C_a(t_s) \frac{K_i}{K_{bld}-K_i} \left[e^{-K_i(t-t_s)} - e^{-K_{bld}(t-t_s)} \right], \qquad (4)$$

where $RC_i(t)$ is the estimated recirculation correction for compartment i at time t. Initial clearance rates (K_i) can be estimated from a curve-stripping of the initial $C_i(t)$ data.

After correction for recirculation is made, tissue clearance rates are reestimated and used in a second derivation of the recirculation correction. Similar corrections can be made if biexponential blood clearance is assumed. Fast and slow clearance rates (K_i) can then be derived from curve-stripping analysis of the corrected log $C_i(t)$. On the basis of known partition coefficients (λ_i) and the derived clearance rates (K_i), flow in the fast and slow compartments is estimated.

Buildup (Washin) Analysis

Since the biophysical aspects of the buildup and clearance of inhaled xenon are virtually the same, a similar analysis can be used for both. However, if one is interested predominantly in fast compartment flow, in vivo "autoradiography" (buildup technique) [8, 12–15] can be used to estimate flow in various regions of interest. Xenon concentration in arterial blood during buildup can be assumed exponential or can be approximated by a step function [14]. In the latter case:

$$C_i(t) = \lambda_i C_a(\max) \left[1 - e^{-K_i(t-t_s)}\right], \qquad (5)$$

where t_s is the time of the proposed immediate blood saturation (chosen to be 0.75 min) after initiation of xenon inhalation.

Using known or empirically measured gray matter partition coefficients (method follows), the buildup rate (K_g) and, hence, the flow rate (f_g) can be estimated. Buildup rates (K_g) were estimated using both curve-fitting and "autoradiography" methodologies. For the latter, a single point during the 2.5–3 min time interval was used.

Brain:Blood Partition Coefficient

The spatial resolution of CT permits the selection of known anatomic areas to approximate the weight factor (w) and thus directly estimate the brain:blood partition coefficient (λ) with a negligible correction for the specific gravity. If equilibrium between the arterial blood and the selected brain region can be assumed:

$$\lambda = \frac{\Delta CT\#_{brain}(\text{at equilibrium})}{\Delta CT\#_{blood}(\text{at equilibrium})}. \qquad (6)$$

The equilibrium is affirmed by obtaining consistent CT enhancement in the blood and brain on serial CT scans performed during prolonged xenon inhalation. In gray matter locales, equilibrium can be assumed after 5 min of xenon inhalation. On the other hand, the partition coefficient in white matter (λ_w) can be estimated by extrapolating to saturation the curve derived from a selected neuroanatomic locale (white matter region) on serial scans performed during 15 min of xenon inhalation and then dividing this number ($\Delta CT\#$ white matter at equilibrium) by the enhancement obtained in the saturated arterial blood ($\Delta CT\#$ arterial blood).

Results

Successful xenon studies were performed in all eight animals with only minor difficulties. The vital signs and arterial blood gases remained stable throughout the procedures. No adverse reaction to xenon was noted in any of the baboons and they all returned to their normal neurologic status.

Equilibrium

Only a minimal amount of xenon was present within the arterial blood in the initial 20 sec of inhalation. After this,

however, the blood rapidly approaches equilibrium within 60–90 sec. The gray matter generally approaches saturation within 5 min, while white matter equilibrium may take as much as 30 min. When an 80% xenon mixture was inhaled, the arterial blood at equilibrium was found to enhance 11–16 CT units (AS&E scanner), the gray matter 10–15 CT units, and the white 15–23 CT units. A larger signal (~10%) could have been obtained if an open ventilation system had been used. However, the cost of xenon gas outweighed the possible gain in signal.

System Stability and Xenon Escape

The average nonenhanced CT number from any selected brain region (30–320 mm^3) imaged sequentially under different heat-loading conditions and at various time intervals was of adequate consistency. The standard error for each of five brain regions evaluated was less than 0.9 CT units. Repeated scanning of the same blood-filled syringe over a 4 min period showed no significant alteration in the derived CT number, indicating a negligible escape of xenon during the short delay (about 12 sec) between blood drawing and scanning.

Visual Observations

The differential enhancement of the gray versus the white matter derived by numerical analysis was also apparent using gross observations (figs. 1 and 2). In the early stages of inhalation, xenon enhancement was prominently visualized in gray matter locales (fig. 3), while the continued inhalation of the inert gas caused greater enhancement in white matter regions. Gross patterns of xenon clearance were also evident after the discontinuation of inhalation. Visual inspection was used to define gray or white neuroan-
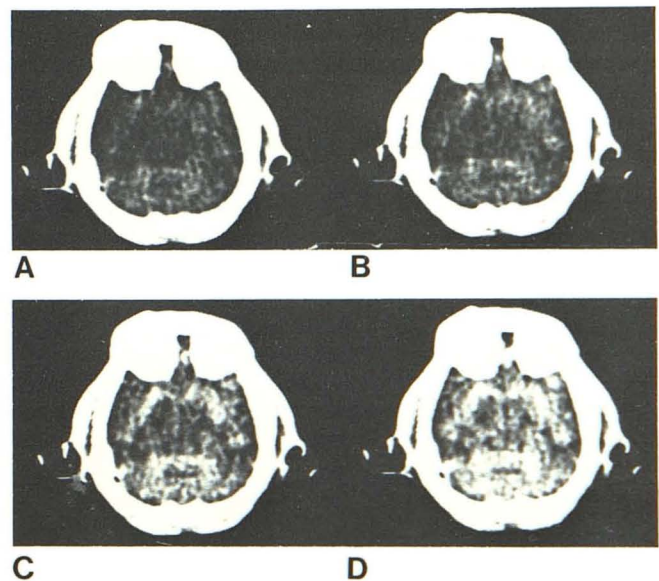

Fig. 1.—Stable xenon buildup. Serial CT scans in baboon at level of midbrain, cerebellum, and temporal lobe during constant inhalation of 80% xenon. Baseline scan (A) compared with scans 1 (B), 2 (C), and 3 (D) min after initiation of xenon inhalation. Prominent, progressively increasing brain enhancement readily noted.
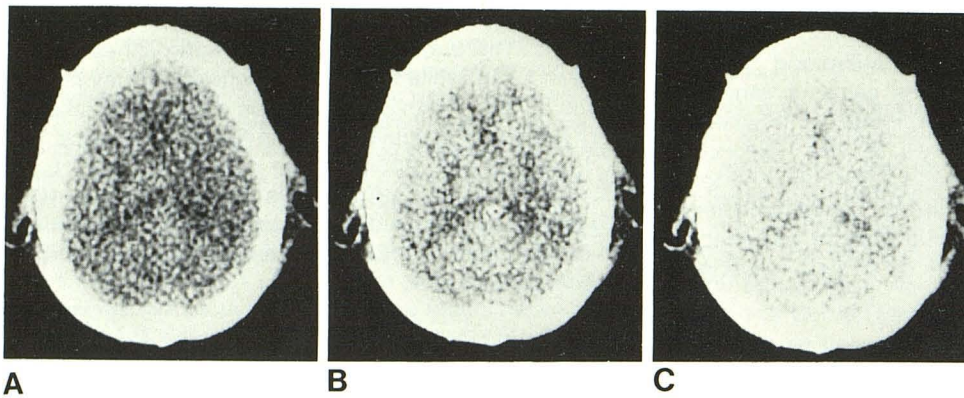
Fig. 2.—Serial xenon CT, frontal horn level. Baseline image (A) compared with scans 2 (B) and 5 (C) min after initiation of xenon (80%) inhalation. Delayed enhancement of internal capsule region as compared with predominantly gray matter structures.

Fig. 3.—Serial CT, xenon buildup (in vivo "autoradiographic" map). CT scans before (A, baseline) and 3 (B) and 6 (C) min after start of 80% xenon inhalation at level just above bodies of lateral ventricles; measure mode photography used to accentuate visualization of brain enhancement. B, 3 min scan. Enhancement occurs primarily in gray matter. C, 6 min. Both gray and white matter are similarly enhanced.

atomic locales and thus estimate the weight factors (w) for flow calculations.

Clearance

Quantitative analyses using the clearance methodology were performed in at least two areas in each of the eight baboons. Typical enhancement in a "gray matter" region chosen by visual inspection and the measured enhancement in the arterial blood is given in figure 4. The arterial xenon concentration in blood was approximated by either a mono- or biexponential clearance function. Typical blood clearance rates were 1.2 min^{-1} with a range of 1.0–1.4 min^{-1}. Since the blood clearance was extremely slow (K blood $= 0.2$ min^{-1}) in the baboon with moderate restrictive lung disease, the brain tissue clearance basically followed the blood clearance, and it was therefore impossible to derive meaningful results for the cerebral blood flow.

All clearance analyses were begun 1 min after termination of xenon inhalation. The typical fast compartment flow rate was 82 ml/100 g/min (range, 58–108 ml/100 g/min). The typical slow compartment flow rates was 16 ml/100 g/min (range, 10–22 ml/100 g/min).

In most regions that were preselected as "white" matter, no significant fast flow was indicated from the results. On the other hand, in almost all the areas preselected as "gray" matter, at least two compartments, fast and slow, were observed. We cannot definitively state whether this slow compartment was due to partial-volume averaging with inclusion of adjacent white matter, or due to tissue with slow
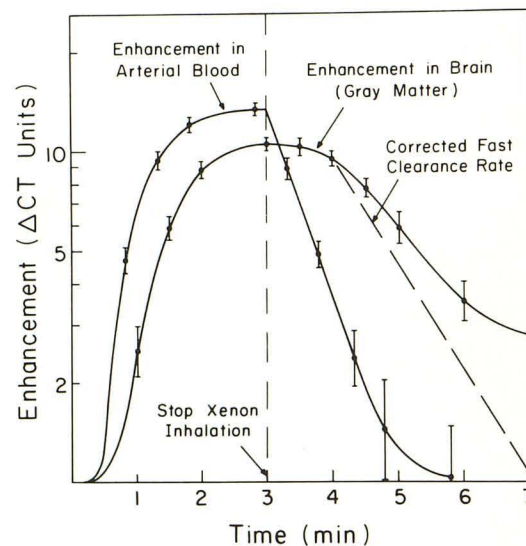

Fig. 4.—Xenon buildup and washout. Idealized curves comparing buildup and clearance of xenon from arterial blood and chosen gray matter locale.

diffusion characteristics in the gray matter. Because of the limited number of data points available in the 1–3 min time interval as compared with the 4–10 min interval and the rapidly changing xenon concentrations in the arterial blood, the overall errors in the derivation of fast and slow flow rates were estimated to be 30% and 20%, respectively.

TABLE 1: **Local Cerebral Blood Flow in One Animal Using In Vivo "Autoradiographic" (Xenon Cerebrogram) Method**

Locale*	Flow Rate Constant, K (min^{-1})	Partition Coefficient, λ	Cerebral Blood Flow Rate (ml/100 g/min)
Frontal Lobe:			
Gray	0.75	0.92	69
White	0.12	1.64†	20
Parietal Lobe:			
Gray	0.64	0.97	62
White	0.08	1.64†	13
Temporal Lobe:			
Gray	0.72	0.95	68
White	0.08	1.64†	13
Cerebellum:			
Gray	0.70	0.95	67
White	0.10	1.64†	16

* Hematocrit, 34; PaCO$_2$, 42.7; 5 min xenon (80%) inhalation.

† White matter partition coefficient (λ = 1.64) was obtained from established hematocrit corrected tables, as only 5 min inhalation was used.

Buildup (in vivo "Autoradiography")

Washin (buildup) quantitative analyses were performed on four normal animals. At least four preselected, predominantly "gray" areas were analyzed in each study. Using the 5 min data point, typical empirically measured, "gray matter" partition coefficients were found to be 0.9 (range, 0.8–1.05). Since the hematocrit measurements of most animals studied were in the low 30s, one would expect a fairly high partition coefficient. However, the question remains whether these numbers are due in part to partial-volume effect with some contribution from "white" matter.

Using a single data point in the 2.5–3.0 min time interval, the buildup rates were calculated on the basis of an assumed monoexponential function for the xenon concentration in the arterial blood as well as a step function. Typical results of fast flow rate constants (K_g) using the in vivo "autoradiography" method were 1.0 min^{-1} (range, 0.7–1.2 min^{-1}).

Fast compartment ("gray") flows derived from the washin technique were 88 ml/100 g/min (range, 60–105 ml/100g/min). We estimate the overall error in derived partition coefficients and flow rates to be 15% and 30%, respectively. Since all clearance analyses indicated multicompartmental flow in "gray matter," a systematic error (5%–10%) in estimated fast flow is introduced by the in vivo "autoradiographic" methodology if a single compartment (fast) is assumed. The results from various brain locales in one animal are presented in table 1.

Discussion

The goal of dynamic studies as such is to generate a functional neuroanatomic map of local rates of cerebral blood flow and blood:brain partition coefficients. Within the expected limitations (described below), the derived flow rate constants (K) and partition coefficients (λ) were consistent, reproducible, and within the expected range for a normal baboon [16]. Heterogeneity of flow [17], both among varying brain locales and within any given locale, was observed in

all animals. In the baboon with moderate respiratory dysfunction, the difficulties were readily apparent from the markedly delayed buildup of xenon concentration in the arterial blood. The in vivo "autoradiographic" (xenon cerebrogram) method seems consistent enough and far easier to perform than the clearance technique. It overcomes many of the potential shortcomings of measuring cerebral blood flow in man with stable xenon and CT scanning (e.g., scanning speed, anesthetic effects of xenon, radiation dose, prolonged patient immobility, single level scanning).

If any of these techniques are to be applied to man, their limitations, advantages, and disadvantages must be understood. The most restrictive limitation of this approach is the biologically limited maximum enhancement that can be achieved during a short period of xenon inhalation. If high concentrations of xenon are used, the anesthetic effects become important within 3 min after initiation of inhalation [18].

Fast scanning, faster recycle time, and improved tube cooling are important if present statistical limitations are to be overcome using curve-fitting techniques. A continuous scan (e.g., 30–60 sec) with the computer capability of breaking down the scan data into numerous segments might prove quite useful. The present method of scanning, namely, single or dual level imaging, limits the volume of tissue chosen for investigation to a relatively narrow slice.

Although CT provides excellent spatial resolution, certain limitations exist when performing quantitative studies. The mean CT numbers are most stable (i.e., smallest standard error) when tissue volumes of 40 mm^3 or greater are chosen for analysis. Compromise decisions must be made concerning the evaluation of even smaller tissue volumes (greater collimation, small cursor size) with increased standard error of the mean CT number yet greater regionality, versus larger tissue volumes (lesser collimation, larger cursor size) with decreased standard error but poorer regionality. Slight variations in patient positioning that seem certain to occur during the 15–20 min required for a clearance study will also have a greater effect on the mean CT number when smaller tissue volumes are analyzed.

The classic signal-to-dose dilemma is of great importance when dynamic CT studies are performed using stable xenon. Although the collimated beam limits the radiated field, repeated scans at the same level result in a significant dose (particularly if repeat studies are to be performed). Many of the limitations described above are lessened when the in vivo "autoradiographic" method is used. However, when this technique is used, the dependence of flow estimates on the accuracy of a single data point becomes a major shortcoming.

The use of arterial blood introduces an additional invasive component into the xenon CT method of measuring cerebral blood flow, although end tidal xenon measurements may be substituted. When arterial blood is scanned, a plastic syringe must be used and great care taken that the scan field includes blood only. Denitrogenation with oxygen is time consuming but not difficult and greatly improves the uptake of xenon by blood at the pulmonary interface.

Despite the many limitations listed above, the spatial

resolution and temporal capabilities of advanced CT scanners permit investigations of local cerebral blood flow in regions of interest with greatly improved tissue specificity. The ability to directly measure the partition coefficient in a relatively small tissue volume, as well as the buildup or clearance rate associated with that specific locale, warrants further investigation of this approach.

From the various methods we have investigated, the in vivo "autoradiographic" technique seems the most promising if xenon-enhanced CT scanning is to be used in man. This is particularly true if our main interest lies in the measurement of "fast" flow. For any given blood enhancement that can be exponentially characterized, an expected level of tissue enhancement may be derived for a normal range of partition coefficients λ_g and buildup rates K_g. In a diseased area, changes in either λ_g or K_g may result in decreased tissue enhancement at a given point in time. The underlying change (i.e., λ and/or K) can then be further characterized by an additional data point (scan) taken later in time. This approach may also allow for multilevel scanning during the 1.5–3.0 min interval when "gray" locales enhance very rapidly as compared to "white." An additional scan at each of these levels during the 4.5–6.0 min interval can be used to define partition coefficients in these areas.

ACKNOWLEDGMENTS

REFERENCES

1. Winkler SS Sackett JF, Holden JE, et al. Xenon inhalation as an adjunct to computerized tomography of the brain: preliminary study. *Invest Radiol* **1977**;12:15–18
2. Drayer BP, Wolfson SK, Reinmuth OM, Dujovny M, Boehnke M, Cook EE. Xenon enhanced CT for analysis of cerebral integrity, perfusion and blood flow. *Stroke* **1978**;9:123–130
3. Zilkha E, Kendall BE, Loh L, Hayward R, Radue EW, Ingren S. Diagnosis of subdural hematoma by computed axial tomography: use of xenon for contrast enhancement. *J Neurol Neurosurg Psychiatry* **1978**;41:370–373
4. Kelcz F, Hilal SK, Hartwell P, Joseph PM. Computed tomographic measurement of xenon brain-blood partition coefficient and implications for regional cerebral blood flow: a preliminary report. *Radiology* **1978**;127:385–392
5. Drayer BP, Wolfson SK, Boehnke M, Dujovny M, Rosenbaum AE, Cook EE. Physiologic changes in regional cerebral blood flow defined by xenon-enhanced CT scanning. *Neuroradiology* **1978**;16:220–223
6. Radue EW, Kendall BE. Xenon enhancement in tumors and infarcts. *Neuroradiology* **1978**;16:224–227
7. Kety SS. The theory and applications of the exchange of inert gas at the lungs and tissues. *Pharmacol Rev* **1951**;3:1–41
8. Kety SS. Measurement of local blood flow by the exchange of an inert, diffusible substance. *Methods Med Res* **1960**;8:228–236
9. Obrist WD, Thompson HK, Wang HS, Wilkinson WE. Regional cerebral blood flow estimated by [133]xenon inhalation. *Stroke* **1975**;6:245–256
10. Kanno I, Lassen NA. Two methods for calculating regional cerebral blood flow from emission computed tomography of inert gas concentrations. *J Comput Assist Tomogr* **1979**;3:71–76
11. Veall N, Mallett BL. Regional cerebral blood flow determination by ^{133}Xe inhalation and external recording: the effect of arterial recirculation. *Clin Sci* **1966**;30:353–369
12. Landau WM, Freygang WH, Rowland LP, Sokoloff L, Kety SS. The local circulation of the living brain: values in the unanesthetized and anesthetized cat. *Trans Am Neurol Assoc* **1955**;80:125–129
13. Freygang WH, Sokoloff L. Quantitative measurement of regional circulation in the central nervous system by the use of radioactive inert gas. *Adv Biol Med Phys* **1958**;6:263–279
14. Eklöf B, Lassen NA, Nilsson L, Norberg K, Siesjö BK, Torlöf P. Regional cerebral blood flow in the rat measured by the tissue sampling technique: a critical evaluation using four indicators C^{14}-Antipyrine, C^{14}-Ethanol, H^3-Water and Xenon[133]. *Acta Physiol Scand* **1974**;91:1–10
15. Sakurada O, Kennedy C, Jehle J, Brown JD, Carbin GL, Sokoloff L. Measurement of local cerebral blood flow with iodo[^{14}C]antipyrine. *Am J Physiol* **1978**;234:H59–H66
16. James IM, Millar RA, Purves MJ. Observations on the extrinsic neural control of cerebral blood flow in the baboon. *Circ Res* **1969**;25:77–93
17. Reivich M, Slater R, Sano N. Further studies on exponential models of cerebral clearance curves. In: Brock M, Fieschi C, Ingvar DH, Lassen NA, Schurmann K, eds. *Cerebral blood flow. Clinical and experimental results*. New York: Springer, **1969**:8–10
18. Morris LE, Knott JR, Pittinger CB. Electro-encephalographic and blood gas observations in human surgical patients during xenon anesthesia. *Anesthesiology* **1955**;16:312–319